Scientia Iranica B (2020) 27(6), 2954–2966

SCIENTIA IRANICA

Sharif University of Technology
Scientia Iranica
Transactions B: Mechanical Engineering
http://scientiairanica.sharif.edu

Research Note

Experimental investigation of the effect of one-dimensional roughened surface on the pool boiling of nanofluids

M. Mohammadi and M. Khayat*

Department of Mechanical Engineering, Science and Research Branch, Islamic Azad University, Tehran, P.O. Box 14515-775, Iran.

Received 4 June 2018; received in revised form 2 March 2019; accepted 2 September 2019

KEYWORDS
Pool boiling;
One-dimensional roughened surface;
Deposition of nanoparticles;
Critical heat flux;
Heat transfer coefficient.

Abstract. This research is aimed at developing a particular surface for promoting nucleate boiling heat transfer characteristics, reducing the superheat temperature and postponing the occurrence of critical heat flux to the long term. To this end, a laboratory apparatus was built. In order to feed the microlayer of bubble more through the capillary force of micro-grooves, the boiling surface was roughened in one direction. Although the boiling characteristics of roughened surfaces were more enhanced than those of the polished surface, the results were not very impressive. Although the boiling of two nanofluids, i.e., copper oxide and alumina, on the micro-groove surface resulted in a significant increase in the nucleate heat transfer coefficient, this method cannot be applied to a process with a long computational time because of continuous deposition of nanoparticles over time and creation of an insulation layer on the micro-groove surface. Therefore, simultaneous utilization of micro-groove surface and deposition of a thin and porous layer of nanoparticles on the surface increased the feeding of sites and production of bubbles, respectively. The critical heat flux and boiling heat transfer coefficients of the surface deposited with copper oxide nanoparticles were enhanced by 46.5% and 74.2%, respectively.

1. Introduction

Electrical systems and equipment are sensitive to heat. The development of materials science and manufacturing technology to reduce the equipment size has attracted the attention of many researchers. Shrinking the size of equipment parts has brought electronic parts closer to each other. Therefore, use of single-phase heat transfer techniques such as usage of fins and blowing the air with fan through fins cannot control the hot spots on the surface and eliminate extreme thermal gradients, which can damage sensitive parts. One of the best ways to meet this demand is to use a two-phase heat transfer technique. The two-phase boiling process involves transferring heavy heat loads from a limited surface with a slight difference in temperatures of the surface and the fluid due to the absorption of the latent heat of evaporation from the surface during the production of bubbles. Conversely, when the received heat flux surpasses Critical Heat Flux (CHF), the steam completely covers the surface and the surface temperature rises sharply due to lower steam conductivity than the base fluid. Finally, the boiling heat transfer characteristics are severely diminished.

Nukiyama in 1934 introduced the concept of boiling and recognized nucleate boiling regions [1]. Aware of this process, researchers have attempted to reduce the superheat temperature of the surface and increase the heat flux and Heat Transfer Coefficient

*. *Corresponding author.*
E-mail address: mkhayat@srbiau.ac.ir (M. Khayat)

doi: 10.24200/sci.2020.51189.2048

simultaneously. Various effective parameters are available to improve the boiling heat transfer characteristics of fluids in low, medium, and high heat fluxes. In addition, some of the most important factors in this regard include early onset of nucleation in low heat flux, increase in the number of active nucleation sites and hydrophilicity of the surface in medium heat fluxes, and postponing the CHF and tearing of insulating bubbles formed on the surface in high heat fluxes [2]. Pournaderi and Pishevar [3] simulated the oblique collision of water droplets with the superheated surface via a novel algorithm. The high temperature of the surface leads to the formation of a vapor layer between the droplet and surface. In this method, mesh clustering near the surface is used to capture the effect of the vapor layer. Available experiments confirmed the validity of the proposed algorithm. The results showed that the Weber number was dependent on the average speed of the collision of the water droplet and also, the drop radius and the contact time of the droplet were dependent on the normal weber number. Rana et al. [4] studied the hydrothermal characteristics of Al_2O_3 and CuO nanofluids subjected to Brownian motion by finite element method. For effective thermal conductivity and effective, viscosity Koo-Kleinstreuer-Li (KKL) model is used. It is observed that the dispersion of nano-particles in Newtonian liquid causes a significant increase in the effective thermal conductivity. In addition to this finding, the effective thermal conductivity of Al_2O_3 nano-liquid was greater than that of CuO nano-liquid. Convection at the surface has notable effect on the temperature of nano liquids. Heat generation through CuO liquid was lower than that in Al_2O_3 near the vicinity of the wall. However, away from the wall, opposite trends were observed. This study considers nanofluids as the best coolant among the base fluids.

Roughening the surface with sandpaper or machining is one of the simplest ways to improve boiling heat transfer characteristics, which may increase the heat transfer coefficient [5–7]. Typically, heat transfer media are composed of fluids such as water, ethylene glycol, or oil and they have a much lower heat transfer coefficient than metals and even metal oxides. Therefore, it is expected that fluids containing very small particles of these compounds show better thermal properties than pure ones. The idea of nanofluids was introduced by Choi and Eastman in 1995, leading to the massive revolution of the field of heat transfer of fluids [8]. Boiling of nanoparticles resulted in some changes in viscosity, surface tension, thermal conductivity, and thermo-physical properties of the suspended particles; besides, deposition of particles on the surface brought about a change in hydrophilicity, roughness, and active nucleation sites of the surface. When the size of the nanoparticles becomes larger, the weighting effect overcomes the diffusion and then, the nanoparticles are deposited. Deposition of nanoparticles whose size exceeds the average roughness of the surface on the cavities not only reduces the density of active nucleation sites and modifies the surface roughness, but also increases the wettability and nutrition of nucleation sites [9].

Wen and Ding [10] performed a pool boiling test using water-alumina nanofluid under atmospheric conditions. They found a considerable improvement of heat transfer upon increasing the concentration of nanoparticles. Das et al. [11] used copper oxide and water-alumina nanofluids to investigate the natural convection heat transfer of pool boiling. The results showed that depositing nanoparticles on the surface would increase the wettability of the surface, increase the thermal resistance of the surface, and reduce the heat transfer from the hot surface to the cooling fluid. Therefore, the higher concentration of nanoparticles caused a lower Heat Transfer Coefficient (HTC). According to Table 1, many researchers have studied the pool boiling of various nanofluids and presented conflicting results.

Despite many experiments done so far on pool boiling of nanofluids and deposited surfaces, it appears that a combination of deposited nanoparticles, one-dimensional roughened surfaces, and porosity of surfaces has never been considered. Based on the contradictory findings of previous studies, in this study, the pool boiling test was carried out to clarify the effects of deposition, material, and size of nanoparticles on HTC and CHF.

In this study, initially, the boiling test was performed using a roughened surface in one direction and Deionized water fluid under a condition characterized by saturation temperature, atmospheric pressure, and ambient temperature of 23°C; then, the uncertainty analysis of extracted results was carried out. Alumina (alpha series) and copper oxide nanoparticles with the average particle sizes of 30 nm and 10 nm and the identical 0.1% vol. concentrations were stabilized using a magnetic stirrer in the ultrasonic process. Using this two-step method without a surfactant ensures the stability of nanoparticles up to 168 hours. A pool boiling test was conducted in the presence of two nanofluids on the one-dimensional roughened surface. The surface was slowly deposited from low to high heat fluxes by nanoparticles. Given that the presence and boiling of nanofluids cannot be considered as a desirable long-term stability method, after creating a porous layer with appropriate thickness and strength, the nanofluids were drained out of the boiling chamber and the boiling test in the presence of two deposition levels and DI water was performed. Finally, all the extracted results were compared with each other and the best and most enduring state was reported.

Table 1. Analysis of the results obtained by researchers about the effect of pool boiling of nanofluids on heat transfer characteristics.

Year [Ref.]	Nanofluids	Concentration	Particles size (nm)	Surface analysis	HTC	CHF
2007 [14]	TiO_2/water Al_2O_3/water	10^{-5} – 0.1 vol%	23 47	SEM	—	75% Enhance 100% Enhance
2008 [15]	ZrO_2/water	0.005–0.15 vol%	20–25	Profilometer	Enhance in low and deteriorated in high concentration	—
2009 [16]	TiO_2/ R141b	0.01-0.03–0.05 vol%	21	Profilometer	Deteriorated	—
2010 [17]	Cu/water without SDS Cu/water with SDS	0.25-0.5–1 Wt.%	10	SEM AFM	Deteriorated	48% enhancement 75% deterioration
2011 [18]	γ-Fe_2O_3/water	0.1 Wt.%	10	SEM AFM	Deteriorate or enhance related to thickness of deposition	90% enhance
2012 [19]	ZnO/EG	0.5-3.75 vol%	30–50	SEM	22% enhance	Enhance with increase concentration
2015 [20]	rGO/water	0.01–0.3 gr/l	322	XRD SEM FI-IR	—	145-245% enhance
2016 [21]	CNT/water FCNT/water	0.1–0.3 Wt.%	$\emptyset(10-20nm)\times$ $L(1.5-2\mu m)$	TEM XRD SEM	Deteriorated	Enhancement

2. Setup of pool boiling apparatus

The image of the boiling apparatus is shown in Figures 1 and 2. The boiling chamber of this device is made up of cylindrical borosilicate glass with dimensions of 300 × 200 × 5 mm, which is highly resistant to high thermal stresses. In addition, this cylinder is completely transparent and provides conditions for

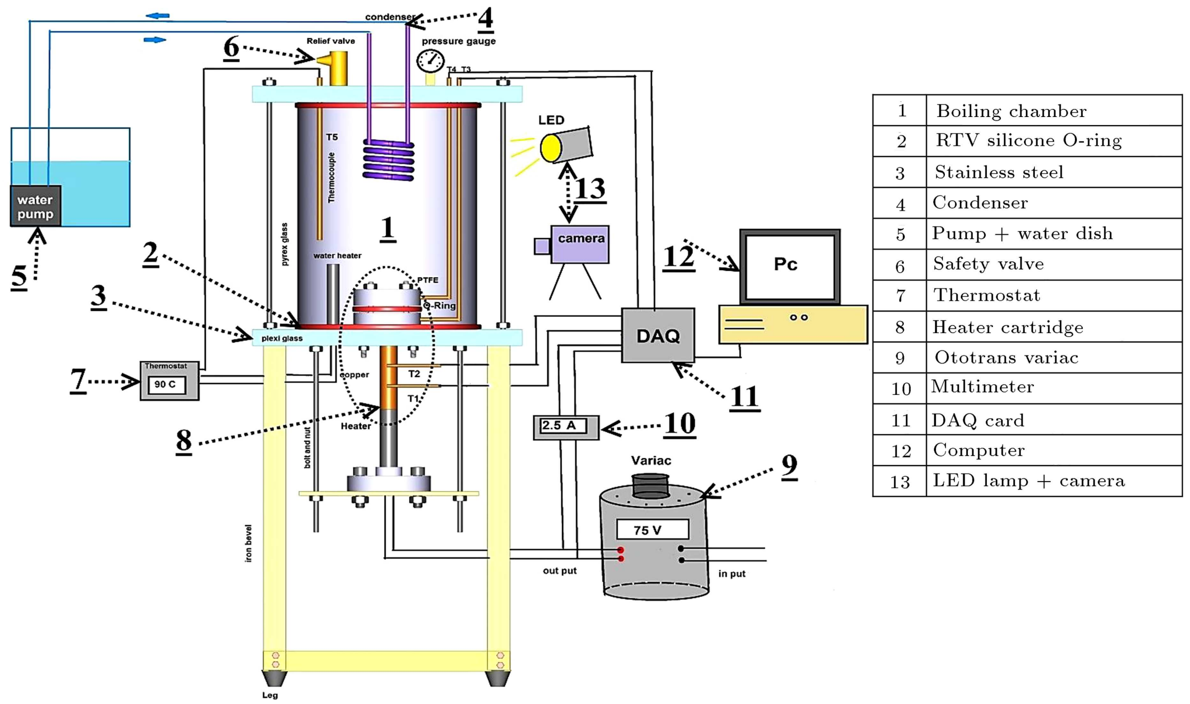

Figure 1. The schematic image of the pool boiling apparatus.

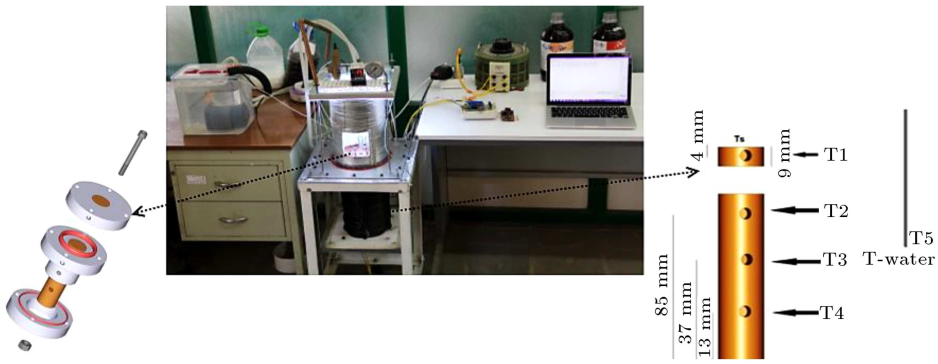

Figure 2. Pool boiling apparatus and position of the sensors in the heater cartridge.

taking pictures of its boiling. This Pyrex chamber is connected to two stainless steel plates by silicone O-ring from the top and bottom, while it is completely sealed by room temperature vulcanizing silicone adhesive sealant. In order to keep the volume and concentration of the nanofluid constant, a copper spiral condenser was used to condense the vapor generated by boiling inside the boiling chamber. The condenser was connected by a hose to water pump, which was located inside a reservoir of cool fluid that formed a closed condensation cycle. A pressure gauge was used to control the pressure inside the boiling chamber, and a safety valve was used to restore the pressure inside the reservoir through the discharge of excess steam into the environment. Moreover, to control the temperature and keep the boiling fluid in saturated conditions, a thermostat connected to the sensor and a water heater was used. The heater cartridge manufactured by computer numerical control machining process with a thickness of 40 mm, height of 250 mm, and boiling surface diameter of 23 mm was made of copper for its high thermal conductivity. Four RTD-Pt100 resistance sensors with a precision rate of $\pm 0.1^{\circ}$C, thickness of 5 mm, and length of 11.5 mm were installed on the cartridge after being calibrated in a constant temperature bath. To achieve better heat transfer between the cartridge body and sensors, the silicon silver paste with thermal conductivity of 4.5 W/m°K was used. In order to exclude radial heat transfer from the cartridge to the environment, the heater cartridge was completely covered by a combination of thermal insulation such as fiberglass, wool and Poly Tetra Fluoro Ethylene (PTFE) insulation. The cartridge was finally connected to a 1500 W heater. Likewise, by using a 3000 W Ototrans, connected to a multimeter, the power of the heater increased gradually. The extracted data from the Resistance Temperature Detector (RTD) sensors were transferred to a data acquisition system and categorized by means of a computer. Additionally, to take pictures of different regions of boiling, the LED lamp and a high frame-rate camera were used.

3. Results

The study consists of six experiments, polished and one-dimensional rough surfaces, one-dimensional rough surfaces in the presence of nanofluids, one-dimensional rough surfaces filled with the nanoparticles. Surface morphology scanning and hydrophilic test of all surfaces and particle diffusion test were carried out.

3.1. Boiling test on clean surface

After machining the boiling surface, the copper surface was perfectly roughened by 600-grit sandpaper in one direction, while the average roughness was 0.114 μm. In order to remove fat and contamination from the surface, the boiling surface was completely cleaned with linen acetone-impregnated tissue. The boiling test was performed on the smooth and roughened surfaces in the presence of DI water as a working fluid, as shown in Figures 3 and 4. These figures show the comparison of the obtained results. The surface morphology analysis using Scan Electron Microscope (SEM) images in Figure 5 (case A) confirmed that the

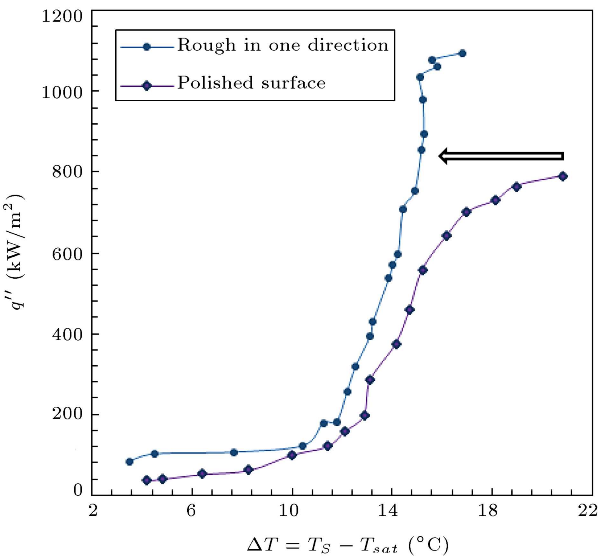

Figure 3. Heat flux according to surface temperature difference.

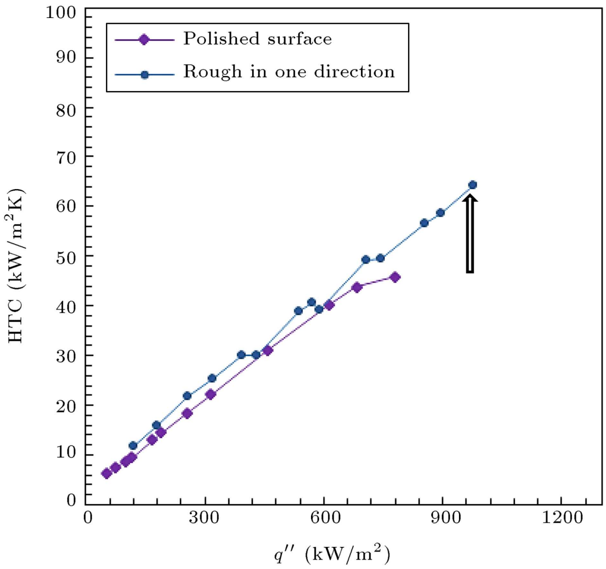

Figure 4. Heat transfer coefficient according to heat flux.

motion of the sandpaper was entirely in one direction; however, the roughened surface has few nucleation sites and porosity. Subsequently, the amount of wettability of the boiling surface was measured by using the droplet static contact angle with the surface. According to Figure 6 (case A), the results showed that due to low surface porosity and capillarity, the drop had a slight tendency to extend to the surface and contact angle was approximately 75°. Hence, lower nucleation sites were fed by fluid. This problem was partly resolved by creating parallel micro-grooves on the surface that could, by their own capillary force, bring nearby fluid underneath the bubble microlayer. At a lower temperature different from that of the polished surface, the CHF and HTCs reached 1095 kW/m^2 and 62 kW/m$^{2\circ}$K, respectively. A few nucleation sites are active and produce bubbles in low heat fluxes. Moreover, the geometric shape of the cavities keeps the bubbles within the sites of the jet so that they often collide and merge with each other on the boiling surface and produce large bubbles, as seen in Figure 7, hence a clean surface.

3.2. *Data extraction method and uncertainty analysis*

Since the heater cartridge is completely covered by a combination of thermal insulation materials, radial heat transfer can be ignored. In other words, heat transfer should be considered as one dimensional and in the axial direction. Figure 2 shows the position of the sensors inside the cartridge. By fitting the internal temperatures of the heater cartridge in different heat fluxes in Figure 8, it was found that curves deviation in all heat fluxes was close to 1. This is the reason why the temperature distribution function can be assumed

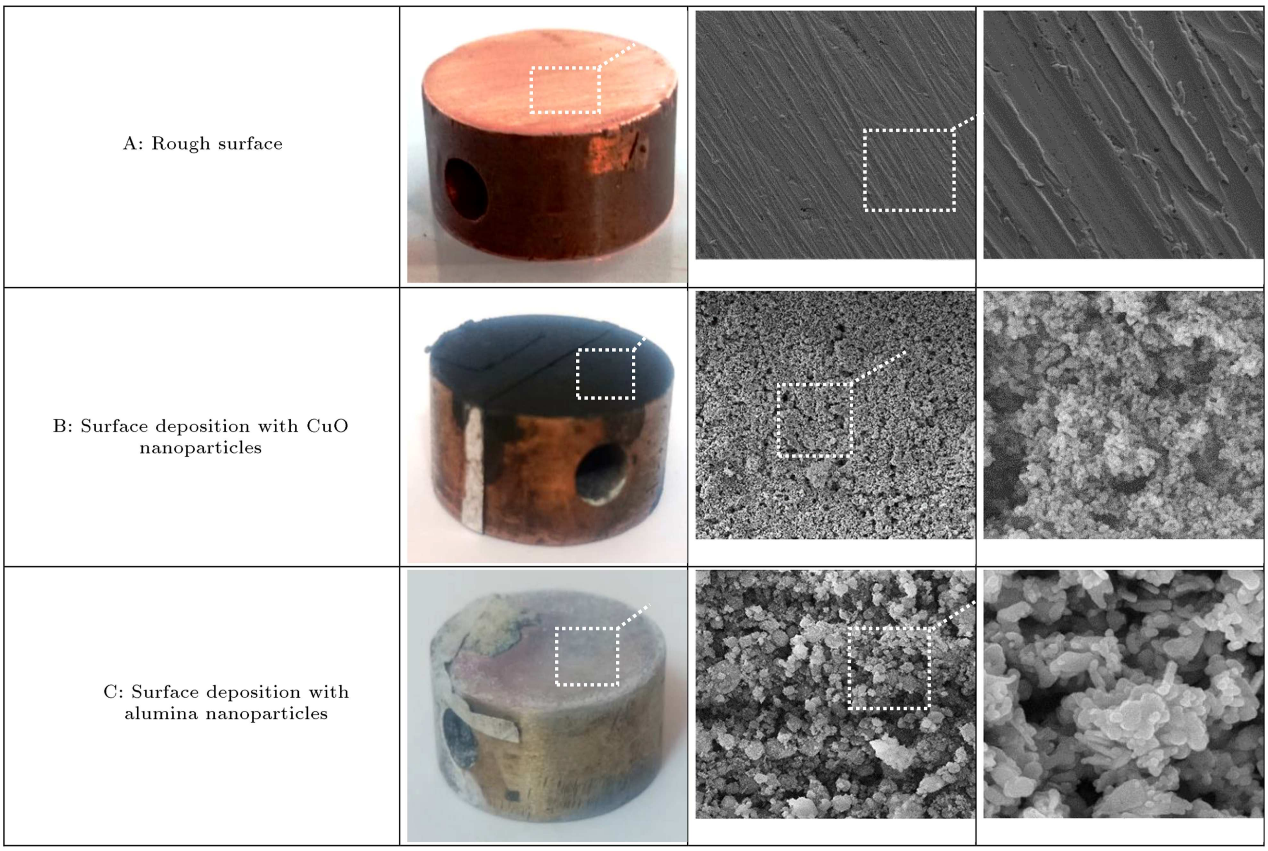

Figure 5. Scan Electron Microscope (SEM) images taken from rough and deposited surfaces.

Surface	Contact angle	Image
A: Clean surface with water droplet	$\theta = 75°$	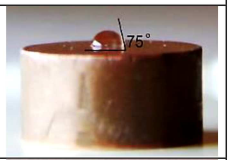
B: Clean surface with CuO droplet	$\theta = 60°$	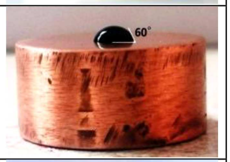
C: Clean surface with Al_2O_3 droplet	$\theta = 50°$	
D: Deposition CuO nanoparticles on surface with water droplet	$\theta = 150°$	
E: Deposition Al_2O_3 nanoparticles on surface with water droplet	$\theta = 10°$	

Figure 6. Static contact angle test for different states.

linear. The heat flux can be calculated using the Fourier one-dimensional heat transfer relationship:

$$q'' = -k\frac{\partial T}{\partial Z}. \tag{1}$$

The value of the heat flux calculated through Eq. (1) was assumed constant. Therefore, the boiling surface temperature can be estimated using expansion of Fourier's law between sensor 1 and boiling surface.

$$T_S = T_1 - \frac{q''d}{k}. \tag{2}$$

By calculating the boiling surface temperature through Eq. (2) and measuring the boiling fluid temperature by sensor 5, the HTC can also be measured using Newton's law of cooling in Eq. (3) ($\Delta T = T_S - T_{sat}$):

$$h = \frac{Q/A}{\Delta T}. \tag{3}$$

Errors are the main factors causing the difference between the calculated and actual values. Human factors or lack of calibration of equipment and parts cause errors. By applying the Holman method, error propagation (Eq. (4)) and uncertainty analysis were implemented [12]:

$$U = \left[\sum_{i=1}^{J}\left(\frac{\partial r}{\partial X_i}\right)^2 U_i^2\right]^{\frac{1}{2}}, \tag{4}$$

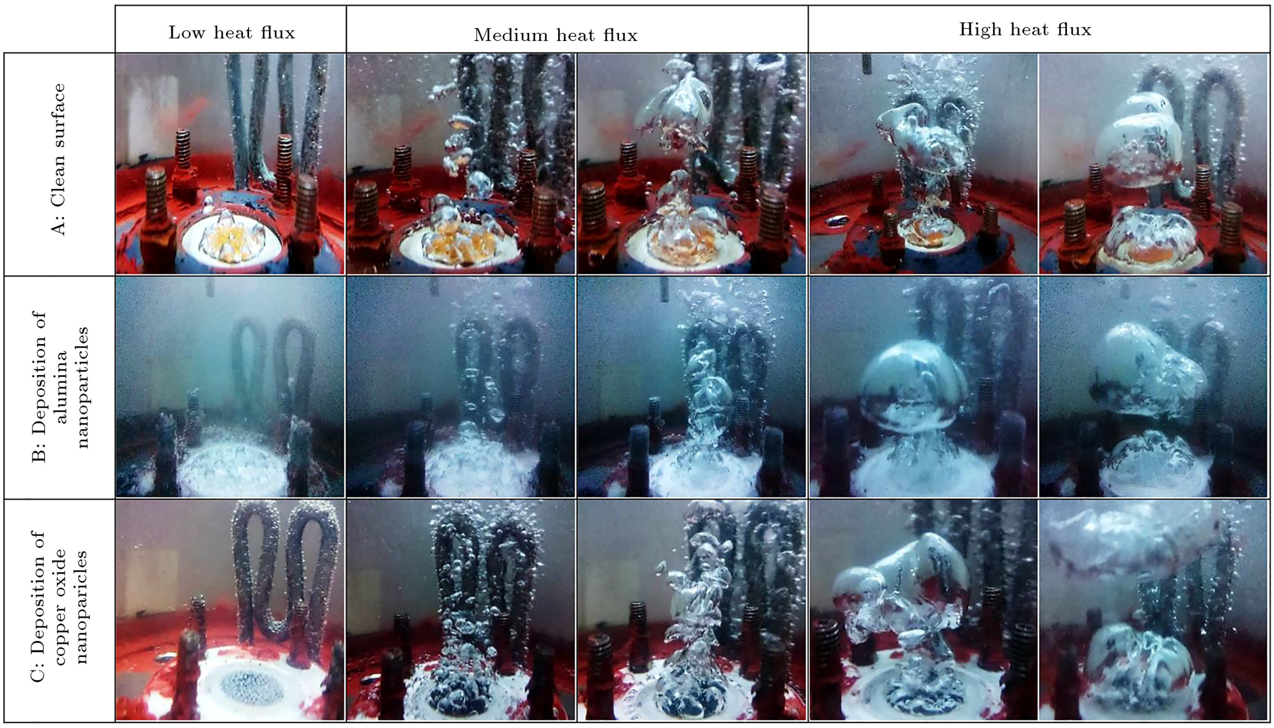

Figure 7. How to form bubbles on rough and deposited surface with nanoparticles.

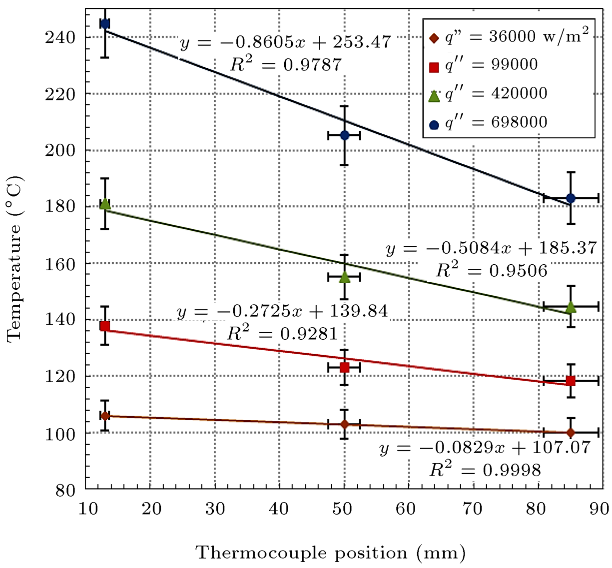

Figure 8. Temperature variations in the heater cartridge in different heat fluxes.

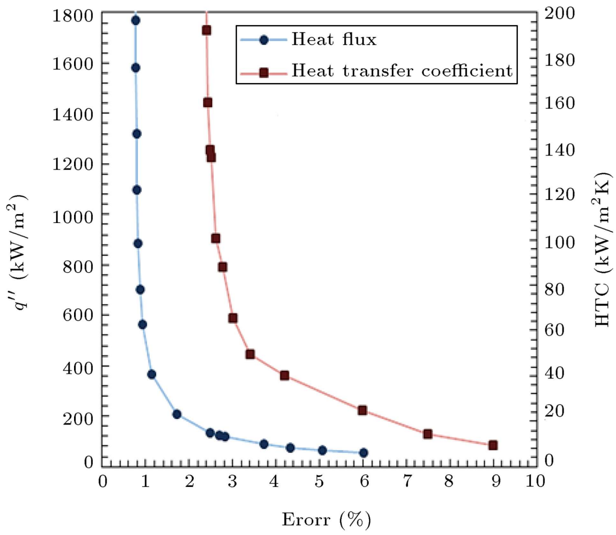

Figure 9. The error rate of the heat transfer characteristics with increasing heat flux.

$$\frac{U_{q''}}{q''}=\sqrt{\left(\frac{U_{T_4-T_1}}{T_4-T_1}\right)^2+\left(\frac{U_{Z_4-Z_1}}{Z_4-Z_1}\right)^2}, \qquad (5)$$

$$\frac{U_{\Delta T_S}}{\Delta T_S}=\sqrt{\left(\frac{U_{T_1-T_{sat}}}{T_1-T_{sat}}\right)^2+\left(\frac{U_{Z_1}}{Z_1}\right)^2}, \qquad (6)$$

$$\frac{U_h}{h}=\sqrt{\left(\frac{U_{q''}}{q''}\right)^2+\left(\frac{U_{\Delta T_S}}{\Delta T_S}\right)^2}. \qquad (7)$$

Based on the accuracy of the measuring device and using the Holman method from the expanded Eqs. (5) to (7), the maximum calculation error of heat flux and HTC reached 6.3% and 9%, respectively. Slight distance of thermocouples from each other and the slight differences in their temperatures increase uncertainty. Increasing the heat flux causes an increase in the temperature difference; hence, the uncertainty percentage decreases (Figure 9). In heat fluxes greater than 500 kW/m^2, the uncertainty percentages associated with the calculation of heat flux and HTC are reduced to values less than 1.4% and 2.81%, respectively.

3.3. One-directional roughened surface in the presence of nanofluids

Copper oxide and alumina nanoparticles were used to improve the heat capacity of the base fluid and overcome the problem of porosity deficiency on the surface. By the same token, 3 liters of 0.1% vol. nanofluids were produced from both nanoparticles. No surfactants or other reactants were used to stabilize the nano-fluid because utility of these additives caused several problems such as reducing the effective particle surface during the heat transfer, instability at high temperatures, and production of foam, which could weaken the heat transfer process [13]. In order to eliminate adhesion of nanoparticles to each other and to achieve uniform distribution of nanoparticles in the base fluid, the nanofluid was initially blended using a magnetic stirrer for 4 hours and then, it was exposed to ultrasonic waves for 3 hours. Finally, the mentioned nanofluid remained in a stable condition for a week. To verify the purity and quality of the purchased particles, both nanoparticles were tested by X-Ray Diffraction (XRD), as shown in Figure 10. The XRD patterns of nanoparticles were found consistent with other particle-diffusion images. Transmission Electron Microscopy (TEM) test demonstrated that alumina and copper oxide nanoparticles had nearly spherical geometries, whose average diameters were 32 nm and 10 nm, respectively. In the presence of nanoparticles, pool boiling test was carried out on a one-dimensional roughened surface, resulting in the patterns shown in Figures 11 and 12. The application of Al_2O_3 nanofluid achieved CHF and HTC values of 1615 kW/m^2 and 73 kW/m^2°K, respectively, in pool boiling test. Similarly, the usage of CuO nano-fluid achieved CHF and HTC values of 1771 kW/m^2 and 80 kW/m^2°K, respectively. An increase in CHF and HTC characteristics relative to the test of the DI water can be attributed to the presence of metal oxide nanoparticles inside the base fluid. In the bubble micro layer, due to continuous evaporation of the working fluid, the fluid volume was reduced. Under these circumstances, the concentration and collision of the nanoparticles increased, facilitating the formation of a thin porous layer of particles on the surface. Moreover, the metallic nanoparticles within the base fluid, especially in the micro layer of the bubble, were inflamed by absorbing heat from the boiling surface. Then, they converted the absorbed energy to the kinetic one by performing

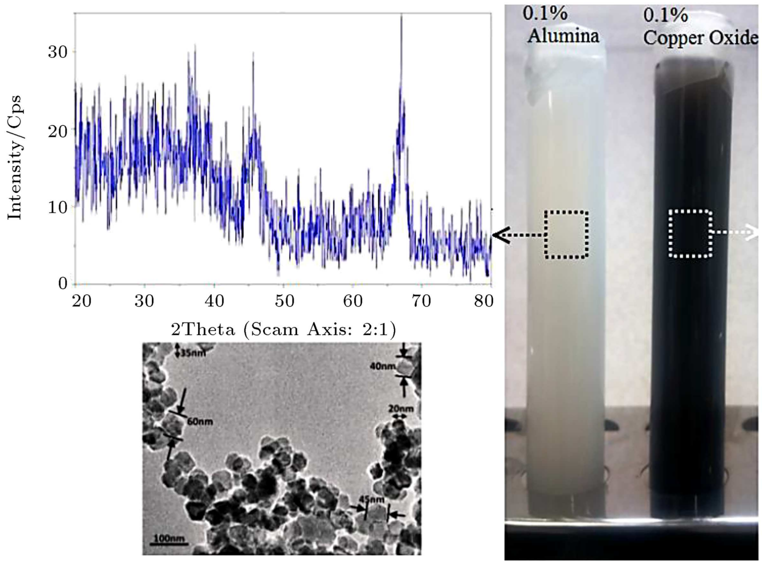

Figure 10. The image of the X-ray diffraction and the Transmission Electron Microscopy (TEM) taken from the nanofluids.

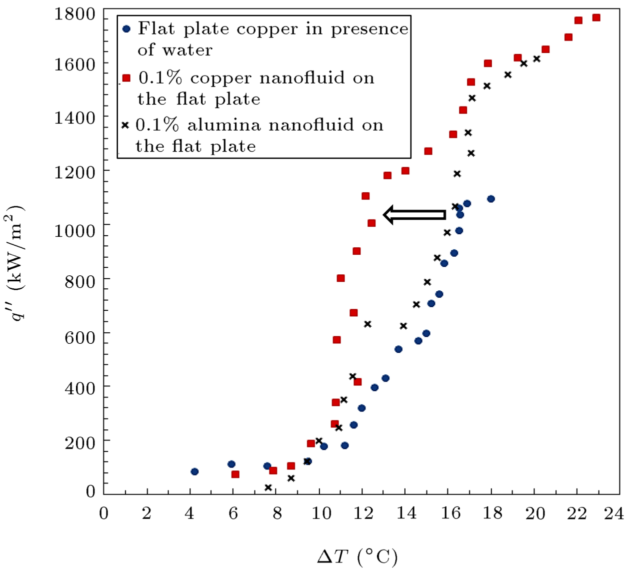

Figure 11. Heat flux according to the surface difference temperature of nanofluids.

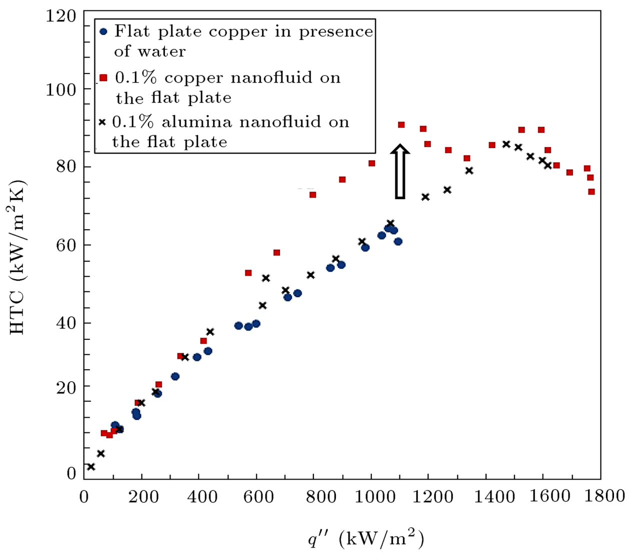

Figure 12. Heat transfer coefficient according to the heat flux of nanofluids.

random movements among the base fluid as well as collision with other particles. When the inflamed particles colliding with large bubbles formed on the boiling surface, the bubbles ruptured faster and the bubble production frequency increased from nucleation sites. The presence of submerged and dispersed nanoparticles within the base fluid extends the effective surface of heat transfer fluid. The nanoparticles constituted shrub-like configuration of the base fluid, transferring heat from the boiling surface to a free surface. The use of copper oxide nanoparticles in comparison with alumina had a greater effect on the increase of HTC and CHF on a one-dimensional roughened surface due to the higher production of nucleation sites as well as smaller particle sizes.

In summary, because the diameter of copper oxide particles is smaller than all nanoparticles used. As a result, these particles, due to heat absorption, produce the ability to move better and also more bubble centers, which causes us to achieve a higher heat flux at a lower temperature difference and the graph is shifted to the left (Figure 11). In the high heat flux near the critical region where large bubbles cover the surface, the results are almost the same for both nanofluids. Figure 6 (cases B and C) shows the static contact angle of the nanofluid droplets on the roughened surface ($50° < \theta < 60°$). Although surface wettability or hydrophilicity is a beneficial factor causing the bubble micro-layer to dry more slowly, the wettability and hydrophilicity of the surface become unfavorable factors in the presence of nanoparticles. As a matter of fact, the higher the level of hydrophilicity, the higher the accumulation of nanoparticles on the sites, causing blockage and reducing the density of active nucleation sites.

3.4. The roughened deposited surface in the presence of DI water

In order to create a strong porous layer with proper thickness on the boiling surface, the nanofluids were boiled for approximately 5 hours from low to high heat fluxes gradually. As a result, the upgraded surface was devoted to thermal indicators such as CHF and HTC, which did not go down over time. The structure of both produced nano-coating surfaces was evaluated by the SEM images, as shown in Figure 5 (cases B and C). The results revealed that the surface deposited by copper oxide nanoparticles grew more at nucleation sites because the diameter of the copper oxide nanoparticles was lower than that of alumina. Deposition of a thin, sponge-shaped layer on the surface produced a super-hydrophilic surface, which is visible in Figure 6, cases D and E. The capillary force of the cavities compels liquid droplets to completely spread on the surface ($10° < \theta < 15°$), hence more feeding of nucleation sites. Figures 13 and 14 were extracted from pool boiling test in the presence of deposited surface and DI-water. In the pool boiling test, the following results were obtained in the presence of the surface deposited by Al_2O_3 and CuO nanoparticles; Al_2O_3: (CHF: 1480 kW/m^2 and HTC: 67 kW/m^2°K) and CuO: (CHF: 1604 kW/m^2 and HTC: 108 kW/m^2°K). Clearly, in constant heat flux, a surface with more nucleation sites, i.e., deposited surface by copper oxide nanoparticles, has a higher HTC in Figure 14. Moreover, as shown in Figure 13, the data of this surface related to roughened surface is shifted to the left, indicating that such a surface has a lower superheat temperature and higher efficiency. Also, due to the production of more bubbles and the release of jet-like bubbles through the cavities (Figure 7), boiling characteristics were enhanced. The sponge-shaped nano-coating deposited on the surface increased the heat transfer of the boiling surface, because both the liquid and the vapor could penetrate the cavities and cool the surface down more efficiently, as can be seen in the schematics of Figure 15.

The presence of parallel micro-grooves on the surface, due to capillary force of the working fluid, forces the fluid to flow through the grooves and feed the high nucleation sites produced by the deposition of nanoparticles. It also delays the drying of the micro-layer bubble. In comparison with the average roughness of the boiling surface, size of nanoparticles is one of the most important factors affecting the number

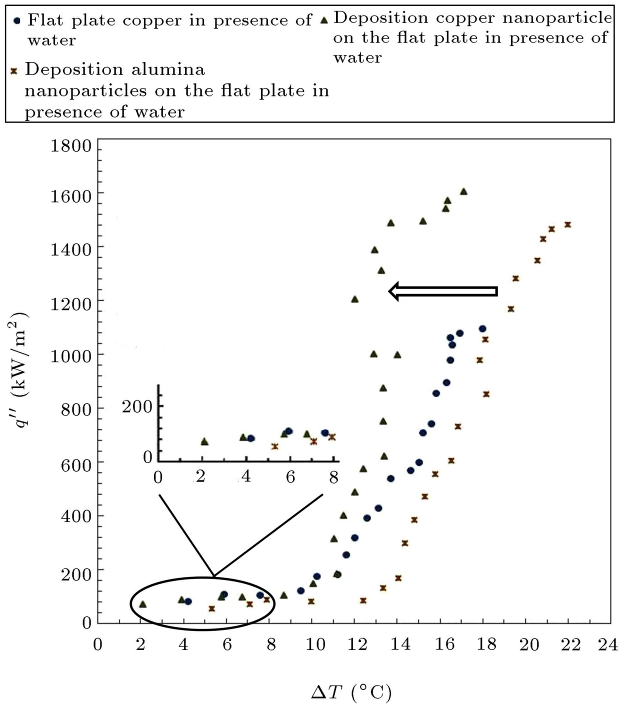

Figure 13. Heat flux according to the surface temperature difference of deposited surface.

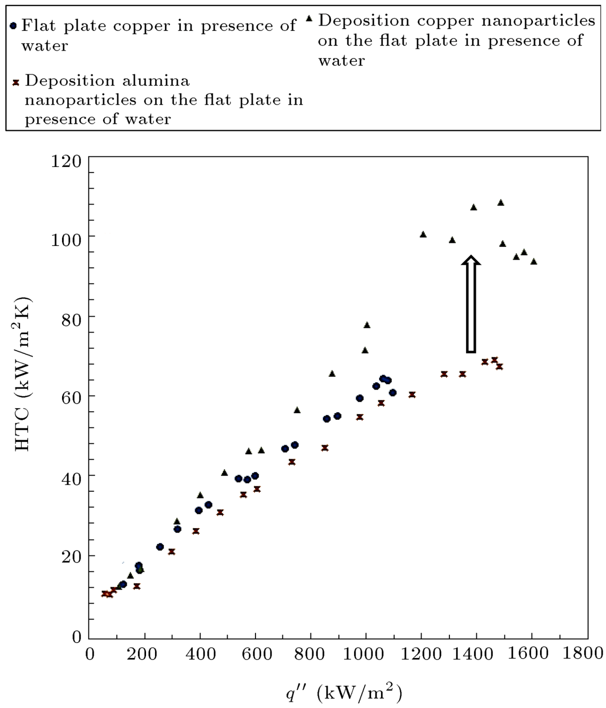

Figure 14. Heat transfer coefficient according to the heat flux of deposited surface.

of nucleation sites and bubble production on deposited surfaces. When the nanoparticle size is smaller than the mean surface roughness, the surface deposited by copper oxide nanoparticles, the entry of these nanoparticles into the grooves creates porosity and

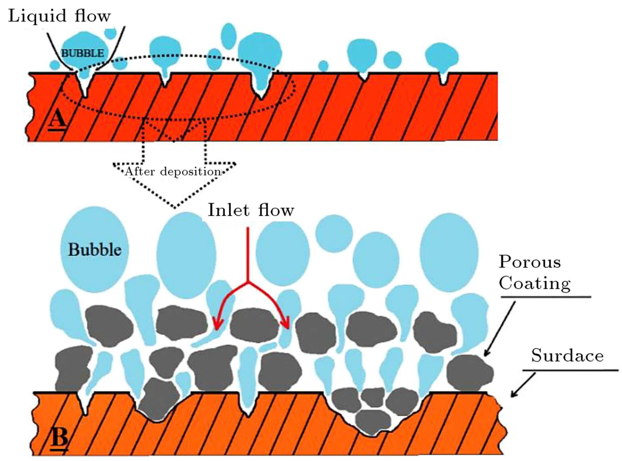

Figure 15. A schematic of bubble formation on two rough and deposited surfaces.

facilitates sponge formation and thus, the movement of fluid from inside the grooves of the surface does not stop. Consequently, a significant increase in the production of nucleation sites is observed. However, compared to copper oxide nanoparticles, the use of alumina nanoparticles due to the larger diameter of the particles leads to a reduction in production of nucleation sites and bubble because of their weaker ability to penetrate into the sites and micro grooves and often deposition on the sites. This phenomenon can be clearly observed in the SEM images (Figure 5) taken from the deposition surfaces.

Since increase in the heat transfer characteristics of the nanofluids was temporary because of the formation of a thick layer of insulation on the boiling surface, the process of increasing the heat transfer characteristics was reversed by time elapsing. Therefore, through the deposition of a sponge layer of alumina nanoparticles and copper oxide on the roughened boiling surface, this process is prevented. The results showed that by using the roughened surface deposited by alumina nanoparticle, the CHF and HTC increased by 35.1% and 8%, respectively. Likewise, by using the roughened surface deposited by copper oxide nanoparticle, the CHF and HTC increased by 46.5% and 74.2%, respectively (Figures 16 and 17). Finally, as shown in Figure 18, the use of copper oxide nanoparticles results in the best performance of the pool boiling heat transfer characteristics due to the smaller average diameter.

3.5. Bubble dynamics in different heat fluxes

The shape of generated bubbles on a roughened surface deposited by alumina and copper oxide nanoparticles is shown in three different heat flux regions in Figure 7. In low heat fluxes, the faster and most activities of nucleation of sites are important. When the surface has higher porosity due to deposition of nanoparticles, especially copper oxide, nucleation sites are more active

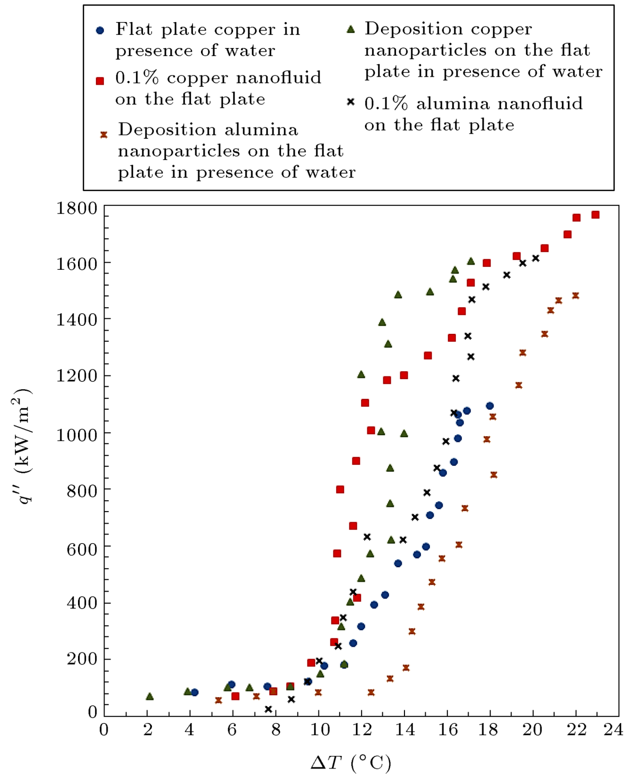

Figure 16. Comparison of heat flux according to the superheated temperature of all states.

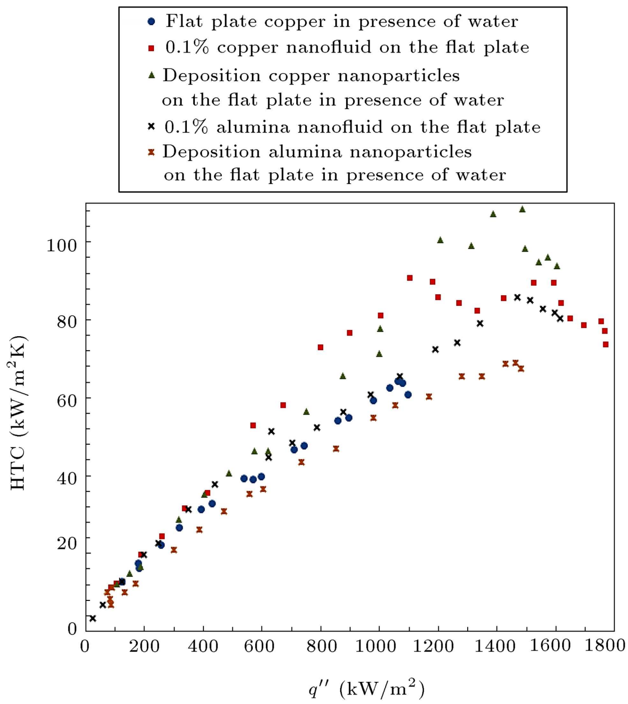

Figure 17. Comparison of heat transfer coefficient according to the heat flux of all states.

at a lower temperature difference (Figures 7 and 13). In medium heat fluxes, the frequency of produced bubbles released from the ordinary surface was low; therefore,

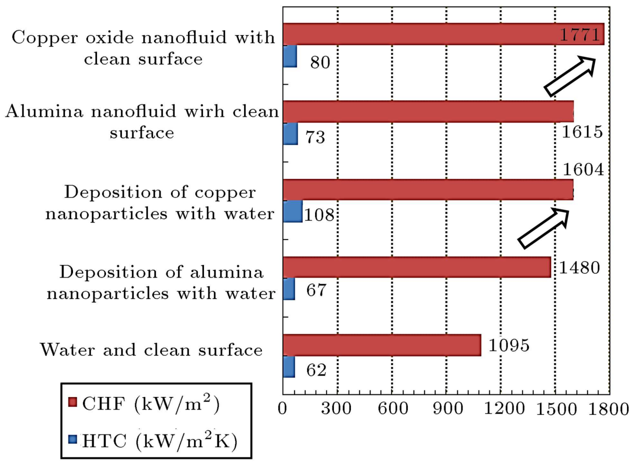

Figure 18. Comparison of heat flux and heat transfer coefficient of all surfaces.

the bubbles have more opportunity for colliding with each other and creating larger mushroom-shaped bubbles on the surface. However, in the same heat flux, the frequency of production and separation rate of bubbles released from the surfaces deposited by nanoparticles, especially copper oxide, were higher due to the smaller diameter of the nano-particles and jet-like bubbles exiting from the sites; thus, the mushroom bubble was not shaped. In high heat fluxes (> 500 kW/m^2), due to the activation of both large and small nucleation sites, small bubbles merged into each other and produced a large bubble, called the dominant bubble. The dominant bubble grew bigger by swallowing other tiny bubbles on the boiling surface. By increasing the buoyant force, the bubble was lifted from the boiling surface and climbed upwards; then, another dominant bubble would be created and replaced by the previous bubble immediately. The diameter of large bubbles formed on the boiling surface is dependent on the density of nucleation sites. Therefore, the diameter of the dominant bubble formed on the surface deposited by copper oxide nanoparticles was larger due to the larger number of nucleation sites (Figure 19). The greater production of dominant bubbles led to the removal of the heat from the surface through the quench mechanism such that the volume of cool fluid above the dominant bubble was replaced and pulled downward. The vortices generated by the upward movement of the bubble caused the cool fluid to flow more quickly into the sites and consequently, increased the production rate of the bubbles.

4. Conclusion

This study aimed to develop an engineered surface suitable for long-term work using the roughened copper surface with a 600-grit sandpaper in one direction. To this end, we have witnessed increasing roughness, trapping the working fluid rather than the polished surface, and creating capillary grooves below the bubbles to feed more nucleation sites; as a result, the values of Critical Heat Flux (CHF): 1095 kW/m^2 and Heat Transfer Coefficient (HTC): 62 kW/m^2°K were achieved, which enhanced the boiling properties of the roughened surface, compared to the polished surface. A one-dimensional roughened surface was used as the base level for other tests.

Alumina (30 nm) and copper oxide (10 nm) nanoparticles were used to produce 0.1% vol. nanofluid due to the limitation of the base fluid heat transfer coefficient and the small number of porosities and nucleation sites on the boiling surface. The results demonstrated that the use of alumina nanoparticles on the roughened surface resulted in a 47.5% increase in CHF and a 17.7% increase in the heat transfer coefficient. Similarly, utilization of copper oxide nanoparticles on the roughened surface resulted in a 61.7% increase in CHF and a 29% increase in the heat transfer coefficient. The use of copper oxide nanoparticles outperformed alumina nanoparticles, because the Brownian motion of the inflamed nanoparticles resulted in a significant increase in the frequency of bubble production due to the collision of the nanoparticles with bubbles and tearing them. This phenomenon was intensified by reducing the particles of the diameter, hence increasing the heat transfer surface and heat transfer coefficient of the base fluids. Moreover, nanoparticles were deposited

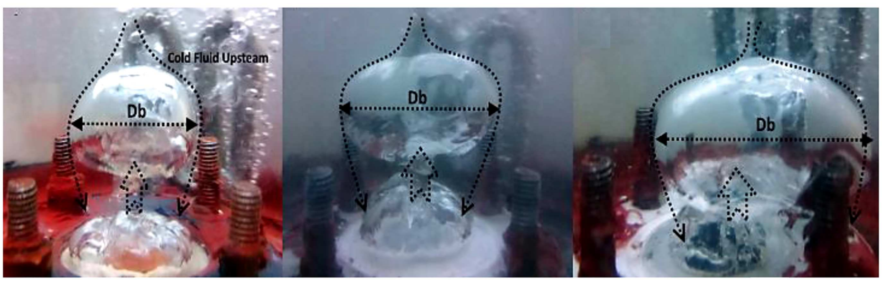

(a) (b) (c)

Figure 19. The diameter of the bubble on the surfaces at high heat flux.

on the boiling surface which facilitated an increase in the production of nucleation sites.

When the nanoparticle size was lower than the average surface roughness, a further increase in the boiling heat transfer characteristics was observed.

The combination of micro-grooves and porosity created a mechanism that increased the nutrition of nucleation sites and a significant increase in bubble production, respectively, which is suitable for long-term work. The change in the bubble dynamics was observed in the low heat flux; faster formation of bubbles and increasing the number of bubbles production were seen in moderate heat fluxes; and in the high heat flux, bubbles did not combine with one another and the CHF was delayed.

Nomenclature

d	Distance between the thermocouple center 1 and the boiling surface (m)
D_b	Bubble diameter (m)
h	Boiling heat transfer coefficient (W/m^{2}K)
K	Thermal conductivity (W/mK)
P	Pressure (Pa)
q''	Heat flux (W/m^2)
Ra	Average roughness (μm)
T	Temperature (K)
T_s	Surface temperature (K)
T_{sat}	Fluid saturation temperature (K)
U	Uncertainty
Z	The position of the thermocouples in the heater cartridge (m)
ΔT	Wall superheat ($= T_s - T_{sat}$) (K)
θ	Contact angle (°)
μ	Viscosity (Ns/m^2)
ρ	Density (kg/m^3)
σ	Surface tension (N/m)

Subscripts

cr	Critical
l	Liquid
S	Surface
sat	Saturation
v	Vapor

References

1. Nukiyama, S. “The maximum and minimum values of the heat Q transmitted from metal to boiling water under atmospheric pressure”, *Japanese Society of Mechanical Engineering*, **9**(12), pp. 1419–1433 (1966).
2. Aznam, S.M., Mori, S., Sakakibara, F., and Okuyama, K. “Effects of heater orientation on critical heat flux for nanoparticle-deposited surface with honeycomb porous plate attachment in saturated pool boiling of water”, *International Journal of Heat and Mass Transfer*, **102**, pp. 1345–1355 (2016).
3. Pournaderi, P. and Pishevar, A.R. “Numerical simulation of oblique impact of a droplet on a surface in the film boiling regime”, *Scientia Iranica*, **21**(1), p. 119 (2014).
4. Rana, Sh., Nawaz, M., and Haider Qureshi, I. “Numerical study of hydrothermal characteristics in nano fluid using KKL model with Brownian motion”, *Scientia Iranica*, **26**(3), pp. 1931–1943 (2019).
5. Kim, D.E., Yu, D.I., Jerng, D.W., Kim, M.H., and Ahn, H.S. “Review of boiling heat transfer enhancement on micro/nanostructured surfaces”, *Experimental Thermal and Fluid Science*, **66**, pp. 173–196 (2015).
6. Kim, J., Jun, S., Laksnarain, R., and You, S.M. “Effect of surface roughness on pool boiling heat transfer at a heated surface having moderate wettability”, *International Journal of Heat and Mass Transfer*, **101**, pp. 992–1002 (2016).
7. Mohammadi. M. and Khayat, M. “Experimental investigation of the effect of roughness orientation of surface on motion of bubbles and critical heat flux”, *Modares Mechanical Engineering*, **17**, pp. 531–541 (2018).
8. Choi, S.U.S. and Eastman, J.A.A. “Enhancing thermal conductivity of fluids with nanoparticles”, in *ASME International Mechanical Engineering Congress* & *Exposition*, San Francisco, CA (1995).
9. Vafaei, S. “Nanofluid pool boiling heat transfer phenomenon”, *Powder Technology*, **277**, pp. 181–192 (2015).
10. Wen, D. and Ding, Y. “Experimental investigation into the pool boiling heat transfer of aqueous based γ-alumina nanofluids”, *Journal of Nanoparticle Research*, **7**, pp. 265–274 (2005).
11. Das, S.K., Putra, N., and Roetzel, W. “Pool boiling of nano-fluids on horizontal narrow tubes”, *International Journal of Multiphase Flow*, **29**(8), pp. 1237–1247 (2003).
12. Holman, J.P., *Experimental Methods for Engineers*, Hill, New York: McGraw-7th Ed. (2001).
13. Amiri, A., Shanbedi, M., Amiri, H., Zeinali Heris, S., Kazi, S.N., Chew, B.T., and Eshghi, H. “Pool boiling heat transfer of CNT/water nanofluid”, *Applied Thermal Engineering*, **71**(1), pp. 450–459 (2014).
14. Kim, H.D., Kim, J., and Kim, M.H. “Experimental studies on CHF characteristics of nano-fluids at pool boiling”, *International Journal of Multiphase Flow*, **33**, pp. 691–706 (2007).
15. Chopkar, M., Das, A.K., Manna, I., and Das, P.K. “Pool boiling heat transfer characteristics of ZrO2-water nanofluids froma flat surface in a pool”, *Journal of Heat and Mass Transfer,* **44**, pp. 999–1004 (2008).

16. Trisaksri, V. and Wongwises, S. "Nucleate pool boiling heat transfer of TiO2-R141b nanofluids", *International Journal of Heat and Mass Transfer*, **52**, pp. 1582–1588 (2009).
17. Kathiravan, R., Kumar, R., Gupta, A., and Chandra, R. "Preparation and pool boiling characteristics of copper nanofluids over a flat plate heater", *International Journal of Heat and Mass Transfer*, **53**(9), pp. 1673–1681 (2010).
18. Stutz, B., Morceli, C.H.S., Silva, M.F., Cioulachtjian, S., and Bonjour, J. "Influence of nanoparticle surface coating on pool boiling", *Experimental Thermal Fluid Science*, **35**, pp. 1239–1249 (2011).
19. Kole, M. and Dey, T.K. "Investigations on the pool boiling heat transfer and critical heat flux of ZnO-ethyleneglycol nanofluids", *Apply Thermal Engineering*, **37**, pp. 112–119 (2012).
20. Kamatchi, R., Venkatachalapathy, S., and Nithya, C. "Experimental investigation and mechanism of critical heat flux enhancement in pool boiling heat transfer with nanofluids", *Heat and Mass Transfer*, **52**(11), pp. 2357–2366 (2016).
21. Sarafraz, M.M., Hormozi, F., Silakhori, M., and Peyghambarzadeh, S.M. "On the fouling formation of functionalized and non-functionalized carbon nano tube nano-fluids under pool boiling condition", *Apply Thermal Engineering*, **95**, pp. 433–444 (2016).

Biographies

Mehdi Mohammadi received his MSc degrees in Mechanical Engineering from the Islamic Azad university of Science and Research Branch, Tehran, Iran (2017). He has conducted extensive research in the field of pool boiling of nanofluids. His major interests include energy conversion, heat and mass transfer, multiphase, and turbulence flows.

Morteza Khayat obtained his PhD in Mechanical Engineering from Sharif University of Technology (SUT), Tehran, Iran. His major interest areas are multiphase flow, heat transfer in porous media, and non-Newtonian fluid flow.